Precision Clinical Medicine, 2024, **7**: pbae026

DOI: 10.1093/pcmedi/pbae026
Research Article

Targeting ESM1 via SOX4 promotes the progression of infantile hemangioma through the PI3K/AKT signaling pathway

Yanan Li,[1,‡] Meng Kong,[1,2,‡] Tong Qiu,[1] Yi Ji[1,*]

[1]Division of Oncology, Department of Pediatric Surgery, West China Hospital, Sichuan University, Chengdu 610041, China
[2]Department of Pediatric Surgery, Children's Hospital Affiliated to Shandong University, Jinan 25002, China
*Corresponding author: Yi Ji, jijiyuanyuan@163.com
‡Yanan Li and Meng Kong contributed equally to this work and share first authorship.

Abstract

Background: Infantile hemangioma (IH) is the most prevalent benign vascular tumor in children, yet its pathogenesis remains incompletely understood. Research has established a strong association between SOX4 and tumor blood vessel formation. The objective of this study was to investigate the function and underlying mechanism of SOX4 in IH development with the aim of identifying novel therapeutic targets.

Methods: We identified the transcription factor SOX4 associated with IH through RNA-seq screening of IH microtumors and validated it in IH tissues. The effect of SOX4 on the biological behavior of CD31+ hemangioma-derived endothelial cells (HemECs) was investigated via *in vitro* cell experiments. In addition, RNA-seq analysis was performed on CD31+ HemECs with low expression levels of SOX4, and the target genes of SOX4 were identified. Finally, the effect of SOX4 on tumor angiogenesis was further elucidated through 3D microtumor and animal experiments.

Results: SOX4 is highly expressed in IH tissues and promotes the proliferation, migration, and angiogenesis of CD31+ HemECs. In addition, SOX4 binds to the endothelial cell-specific molecule 1 (ESM1) promoter to promote the progression of the PI3K/AKT signaling pathway. Finally, through IH 3D microtumor and animal experiments, SOX4 and ESM1 are shown to be tumorigenic genes that independently promote tumor progression.

Conclusions: SOX4 plays a crucial role in the progression of IH, and the SOX4/ESM1 axis may serve as a novel biomarker and potential therapeutic target for IH.

Keywords: infantile hemangioma; CD31+ HemECs; SOX4; proliferation; angiogenesis

Downloaded from https://academic.oup.com/pcm/article/7/4/pbae026/7816374 by guest on 04 December 2025

Received 2 August 2024; revised 22 September 2024; accepted 7 October 2024. published 9 October 2024
© The Author(s) 2024. Published by Oxford University Press on behalf of the West China School of Medicine & West China Hospital of Sichuan University. This is an Open Access article distributed under the terms of the Creative Commons Attribution-NonCommercial License (https://creativecommons.org/licenses/by-nc/4.0/), which permits non-commercial re-use, distribution, and reproduction in any medium, provided the original work is properly cited. For commercial re-use, please contact journals.permissions@oup.com

Graphical Abstract

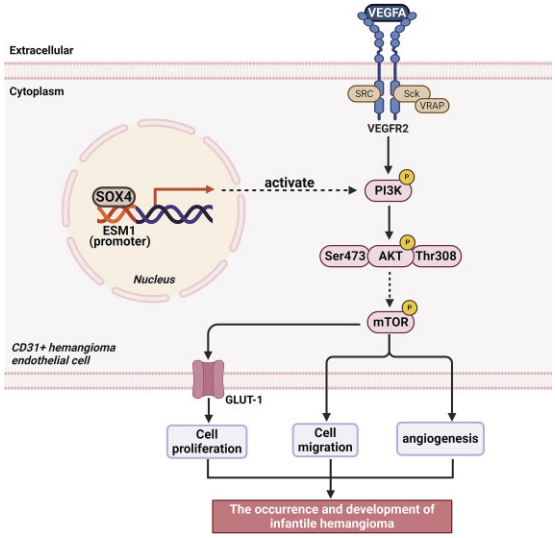

The SOX4 protein in the nucleus of CD31+ HemECs binds to the downstream target gene ESM1, further activating the PI3K/AKT signaling pathway. This activation promotes the migration and angiogenic behaviors of CD31+ HemECs, facilitating the occurrence and progression of IH. In addition, the activated PI3K/AKT signaling pathway upregulates the expression of GLUT-1, which is a biological marker of IH, thereby enhancing cell proliferation and ultimately driving the progression of IH. The SOX4-ESM1 signaling axis may be a potential therapeutic target for IH.

Introduction

Infantile hemangioma (IH) is the most common benign vascular tumor in children, with an incidence of ∼4%–10% [1, 2]. Its prevalence is greater in premature infants and low birth-weight infants, with a male-to-female incidence ratio of ∼1 : 3 [3, 4]. While 90% of IH cases resolve spontaneously, a small percentage may result in permanent pigmentation, fibrous tissue accumulation, and scarring, impacting the aesthetic appearance of children [5]. Some IH cases may be associated with bleeding, pain, infection, and ulcers, which significantly affect the quality of life of affected children [6, 7]. IH occurring in specific locations can lead to severe complications such as organ failure, visual impairment, restricted joint movement, breathing difficulties, and even death [8–10]. Furthermore, IH can have adverse effects on the mental well-being of children and their families [11, 12].

There are notable structural and physiological differences between 2D cell cultures and *in vivo* cells. Moreover, cell suspension-implanted lesions often regress quickly in nude mice, limiting the understanding of IH pathophysiology and progression [13]. Therefore, establishing stable, dependable, and standardized models is crucial for elucidating the detailed mechanisms underlying IH onset and development, identifying new therapeutic targets, and developing novel treatments. In our previous research, we utilized decellularized extracellular matrix from porcine aortas to create a decellularized extracellular matrix micropattern chip to construct a 3D microtumor model of CD31+ hemangioma-derived endothelial cells (HemECs). This approach allows precise control of the size and arrangement of cell clusters, enhancing the authenticity and stability of drug screening and mechanistic exploration [14]. Using this model, we conducted RNA-seq analysis of 3D microtumors and 2D planar CD31+ HemECs. We then performed a joint analysis of the upregulated differentially expressed genes in these cellular models, as well as those identified in our previous RNA-seq results from IH tissues during the proliferating and involuting phases [15]. Through this analysis, we identified the gene SOX4, which may be closely associated with the progression of IH.

SOX4, a member of the SOX gene family, is a crucial and highly conserved transcription factor that encodes an ∼47 kDa protein. It features a highly conserved high mobility box DNA-binding domain with evolutionary conservation, playing a significant role in stable stem cell differentiation, cartilage differentiation, and progenitor cell development [16]. SOX4 is frequently implicated as a retrovirus integration site, leading to mRNA elevation [17]. Research has shown that SOX4 is involved in the differentiation, proliferation, migration, apoptosis, and epithelial–mesenchymal transition (EMT) of tumor cells [18]. Recent studies have highlighted the elevated expression of SOX4 in various malignant tumors, such as glioblastoma, prostate cancer, bladder cancer, liver cancer, lung cancer, and breast cancer, suggesting its potential role in promoting intratumoral neovascularization and tumor progression [19–24]. Numerous studies have demonstrated that SOX4 can modulate several developmental signaling pathways, including the PI3K/AKT, Wnt, and transforming growth factor-beta (TGF-β) pathways, among others, thereby influencing disease progression [25–28]. This finding implies that SOX4 may play a pivotal role in tumor angiogenesis. Despite extensive research on SOX4 in various cancers, studies focusing on SOX4 in IH are limited. The mechanism of action and the transcriptional regulatory network of SOX4 in IH remain unclear. Further exploration is needed to identify the downstream target genes regulated by SOX4 and the signaling pathways involved. Therefore, our study aimed to investigate the impact of SOX4 on IH progression through experiments involving IH tissue samples, 2D planar cells, 3D microtumour models, and animal tumor formation. By elucidating the downstream molecular mechanisms of SOX4 in regulating IH development, we aimed to identify novel targets and obtain insights for the treatment of IH.

Downloaded from https://academic.oup.com/pcm/article/7/4/pbae026/7816374 by guest on 04 December 2025

Materials and methods

Patients and samples

Tissue samples were collected from 16 children who were diagnosed with IH and underwent surgery at the Pediatric Surgery Department of West China Hospital between January 2021 and December 2023. The experimental group consisted of proliferating-phase IH tissue ($n = 10$), whereas the control group consisted of involuting-phase IH tissue ($n = 6$). All the samples were confirmed to be IH via pathological examination via hematoxylin–eosin (HE) staining and glucose transporter albumin 1 immunohistochemistry (IHC) (Fig. S1, see online supplementary material). The clinical data of the children with IHs were obtained surgically at our hospital (Table S1, see online supplementary material).

Antibodies and reagents

Endothelial basal medium (EBM-2) (No. CC-3156, Walkersville, MD, USA), fetal bovine serum (FBS) (No.101Z, New Zealand), phosphate-buffered saline (No. G0002-20 L, Wuhan, China), penicillin and streptomycin (No. JS10835-2, Shanghai, China) were used. Anti-SOX4 antibody (No. CL5634, Cambridge, UK) and anti-endothelial cell-specific molecule 1 (anti-ESM1) antibody (No. ab224591, Cambridge, UK) were used.

Culture and treatment of 2D cells and 3D microtumours

CD31+ HemECs were cultured in endothelial basal medium supplemented with 10% FBS, penicillin (100 U/ml), and streptomycin (100 μg/ml) [29, 30]. Cells were isolated from proliferating-phase IH tissues from three children ($n = 3$). Cultures were maintained at 37°C with 5% CO_2 and 95% humidity. The cells at 90% confluence were dissociated with 0.25% trypsin (No. 25200–056, Beijing, China) and used for experiments from passages 3–8. The 3D microtumour model followed previously described methods [31].

Construction of small interfering RNA (siRNA) and overexpression plasmids

SOX4/ESM1 overexpression plasmids (Tsingke Biotech Co., Ltd., Beijing, China) were constructed (Table S2, see online supplementary material) by amplifying target gene fragments via PCR and inserting them into linearized pcDNA3.4/pcDNA3.1 vectors (oe-SOX4/oe-ESM1). The empty vector was used as a control (oe-NC). siRNAs were purchased and transfected via Lipofectamine 8000TM (No. C0533, Beyotime, China).

IHC/immunofluorescence staining

Paraffin sections (4 μm) were subjected to antigen retrieval and treated with 3% H_2O_2 (No. P0100A; Beyotime, China). After blocking with sheep serum, primary antibodies (1 : 200 dilution) were added, and the sections were incubated overnight at 4°C. Following secondary antibody (1 : 1000 dilution) incubation, the sections were stained with hematoxylin (No. HZ2144, Shanghai, China) and processed for imaging.

Western blot

Total protein was extracted via RIPA lysis buffer (No. P0013B, Beyotime, China), quantified via the bicinchoninic acid method, and transferred to polyvinylidene fluoride membranes (No. FFP19, Beyotime, China). After incubation with primary and secondary antibodies, the membranes were processed for color development.

Quantitative real-time PCR (qRT-PCR)

The target gene sequence was designed via Primer-BLAST software on the basis of the full gene sequence provided by NCBI GenBank, with glyceraldehyde-3-phosphate dehydrogenase (GAPDH) serving as the internal reference. The gene primers used were synthesized by Beijing Qingke Biological Company (Table S3, see online supplementary material). Total RNA was extracted via TRIzol (No. R0016, Beyotime, China). Reverse transcription followed by PCR with SYBR Green (No. HY-K0501A, Shanghai, China) was conducted, and the results were analyzed via the $2^{-\Delta\Delta Ct}$ method.

Cell Counting Kit-8 (CCK-8) assay

The cell suspensions were seeded in 96-well plates, treated with plasmids or siRNAs, and incubated. Cell proliferation was assessed by adding CCK-8 reagent (No. C0037, Beyotime, China) and measuring the absorbance at 450 nm.

5-Ethynyl-29-deoxyuridine assay

The cells were incubated with a 5-ethynyl-29-deoxyuridine (EdU) solution, fixed, permeated, and stained following the kit instructions (No. C0071S; Beyotime, China). Nuclei were stained with DAPI and analyzed by flow cytometry.

Scratch assay

The cells were cultured for 24 h, scratched with a pipette tip, and washed. After incubation with serum-free medium for 24 h [32], the area between cells was analyzed via Image J.

Transwell assay

An 8 μm pore size for migrating cells (No. 3422, Kimble, USA) was used for the migration test. The cells suspensions were placed in the upper chamber and incubated for 24 h in medium supplemented with 10% FBS. After incubation, the cells in the upper compartment were scraped and fixed with Rehsen–Giemsa reagent [33]. The number of cells that migrated through the chamber was then counted under a microscope.

Apoptosis assay

The cells were adjusted to 1×10^6 cells/ml and treated with an Annexin-V-FITC apoptosis detection kit (Bioscience, Shanghai, China). YF647A-Annexin V and propidium iodide (PI) reagents were added to the cell suspension, which was then incubated in the dark for 15 min [34]. Apoptosis analysis was performed via a BD FACSVerse.

Angiogenesis assay

Matrigel (No. C0371, Beyotime, China) was added to a 96-well plate and allowed to solidify. The cells were then added and cultured for 4 h. Blood vessel formation was observed and photos were taken [35]. The number of cell tubes and the length of the main tube were calculated via Image J software.

Microtumor RNA-seq

We extracted RNA from CD31+ HemEC 3D microtumours and 2D planar cells ($n = 3$). Following quality inspection, a library was constructed, and RNA-seq was conducted to identify downstream targeted molecules and signaling pathways associated with SOX4. An Illumina NovaSeq 6000 (Seqhealth, Wuhan, China) was used for sequencing, quantification, and enrichment of products ranging from 200 to 500 bp [36].

Downloaded from https://academic.oup.com/pcm/article/7/4/pbae026/7816374 by guest on 04 December 2025

The database predicted the promoter binding sites of SOX4 and ESM1

The JASPAR database (https://jaspar.elixir.no/), which is maintained by the University of Copenhagen, is a comprehensive open database that updates ChIP-seq data and literature on transcription factor-binding sites. It allows for the prediction of transcription factor-binding sites on the basis of promoter sequences [37]. By searching the database, we selected SOX4 as a potential binding transcription factor (Table S4, see online supplementary material) and obtained the ESM1 promoter sequence in Fasta format from the Scan bar.

Chromatin immunoprecipitation sequencing-PCR

The detailed steps for DNA fragmentation of chromatin via chromatin immunoprecipitation sequencing (ChIP)-PCR are generally as follows [38]. (i) For cell fixation, cells are fixed with 0.75% formaldehyde (No. P0099, Beyotime, China), which typically reacts at room temperature for 10–15 min. After fixation, the reaction was terminated with phosphate-buffered saline. (ii) Cell lysis: the cells are lysed in lysis buffer (buffer containing Sodium dodecyl sulfate (SDS) and protease inhibitors) to release chromatin. (iii) Chromatin fragmentation: chromatin is fragmented via an ultrasonic disruptor or enzymatic digestion. When ultrasound is used, an appropriate power and time are set to obtain DNA fragments 150–600 bp in size. (iv) Impurities should be removed via methods such as centrifugation or ultrafiltration to remove unbroken chromatin and other impurities. (v) Immunoprecipitation: specific antibodies are added for immunoprecipitation to enrich DNA fragments bound to the target protein. (vi) Wash and reverse cross-linking: the immunoprecipitated complexes are washed with wash buffer, and finally reverse cross-linked by heating or other methods to release DNA. (vii) DNA purification: a DNA purification kit was used to remove proteins and other impurities, and purified DNA was obtained for subsequent PCR analysis. These steps ensure effective fragmentation and enrichment of target DNA in ChIP-PCR for further experiments. These target DNA fragments are amplified via specific primers. The ESM1 promoter primer sequence (Table S5, see online supplementary material) was designed via primer-BLAST and synthesized by Beijing Qingke Company. qPCR was performed via a 10 μl SYBR Green system with specific reaction conditions: predenaturation at 95°C for 5 min, followed by 49 cycles of PCR at 95°C for 15 s and 60°C for 30 s. Analysis was performed via the $2^{-\Delta\Delta Ct}$ method.

Experiment for subcutaneous tumor formation in nude mice

Male BALB/c-nude mice (4–6 weeks old) were obtained from Beijing Huafukang Biological Company and housed in a specific pathogen-free laboratory at 22–26°C and 55 ± 5% humidity. After 1 week of acclimatization, CD31+ HemECs were collected, counted, centrifuged, and resuspended. The mice were divided into four groups ($n = 5$): the siRNA/plasmid control group, the low SOX4 group, the overexpressing ESM1 group, and the low SOX4 + overexpressing ESM1 group. The mice were anesthetized and subcutaneously injected in the back with 1×10^7 cells/200 μl (including 100 μl of Matrigel). After 1 week, the mice were euthanized, the tumors were measured and photographed, and the tissue samples were fixed with 4% paraformaldehyde for HE and CD31 IHC staining. Microtumor vessel density (MVD) was calculated via Image J software.

Statistical analysis

The data were analyzed via SPSS version 26.0 software (Chicago, IL, USA). The measurement data are expressed as mean ± standard deviation (SD). Student's t test was used for comparisons between two groups, analysis of variance (ANOVA) was used for comparisons between multiple groups, and Pearson analysis was used for correlation analysis. Statistical significance was set at P values < 0.05.

Results

Screening for the gene SOX4, which may be closely related to the development of IH

RNA-seq of CD31+ HemEC 3D microtumors and 2D planar cells (three samples each) identified 2219 differentially expressed genes (DEGs): 1288 upregulated and 931 downregulated (Fig. S2A and B, see online supplementary material). Additionally, RNA-seq of proliferating- and involuting-phase IH tissues (three samples each) in our preliminary study revealed 374 DEGs: 115 upregulated and 259 downregulated (Fig. 1C and D, respectively) [39]. The intersection of upregulated genes from CD31+ HemECs and IH tissues revealed 10 common genes, including SOX4 (Fig. S2E). A literature review suggested the potential role of SOX4 in IH development. qRT–PCR confirmed greater SOX4 expression in 3D microtumors than in 2D cells (Fig. S2F), indicating the potential role of SOX4 in CD31+ HemEC microtumors.

SOX4 was highly expressed in IH tissues during the proliferating phase

qRT-PCR and Western blot results revealed significantly higher SOX4 mRNA and protein levels in proliferating IH tissues than in involuting-phase tissues (Fig. 1A and B). IHC staining revealed that SOX4 was localized primarily in the nucleus, with stronger expression in proliferating-phase tissues (Fig. 1C). The immunofluorescence results corroborated these findings (Fig. 1D). On the basis of these findings, we speculate that SOX4 may play a role in the development of IH.

SOX4 promotes CD31+ HemEC angiogenesis and the expression of vascular endothelial function-related factors (VEGF-A and matrix metalloproteinase 2)

CD31+ HemECs transfected with SOX4 siRNA and overexpression plasmids were used to establish knockdown and overexpression groups (Fig. S3, see online supplementary material). CCK-8, EdU, scratch, Transwell, apoptosis, and angiogenesis assays revealed that SOX4 knockdown inhibited proliferation, migration, and angiogenesis, whereas SOX4 overexpression promoted these activities (Fig. 2A–M). Western blot analysis revealed that SOX4 knockdown reduced VEGF-A and matrix metalloproteinase 2 (MMP2) protein levels, whereas SOX4 overexpression increased their levels (Fig. 2K and L).

SOX4 may play a role in activating the PI3K/AKT signaling pathway

Western blot analysis revealed that SOX4 knockdown decreased p-PI3K, p-AKT, and p-mTOR levels without affecting total PI3K, AKT, or mTOR levels (Fig. 3A). Conversely, SOX4 overexpression increased p-PI3K, p-AKT, and p-mTOR levels (Fig. 3B). These findings suggest that SOX4 may promote the progression of IH by activating the downstream PI3K/AKT signaling pathway.

Downloaded from https://academic.oup.com/pcm/article/7/4/pbae026/7816374 by guest on 04 December 2025

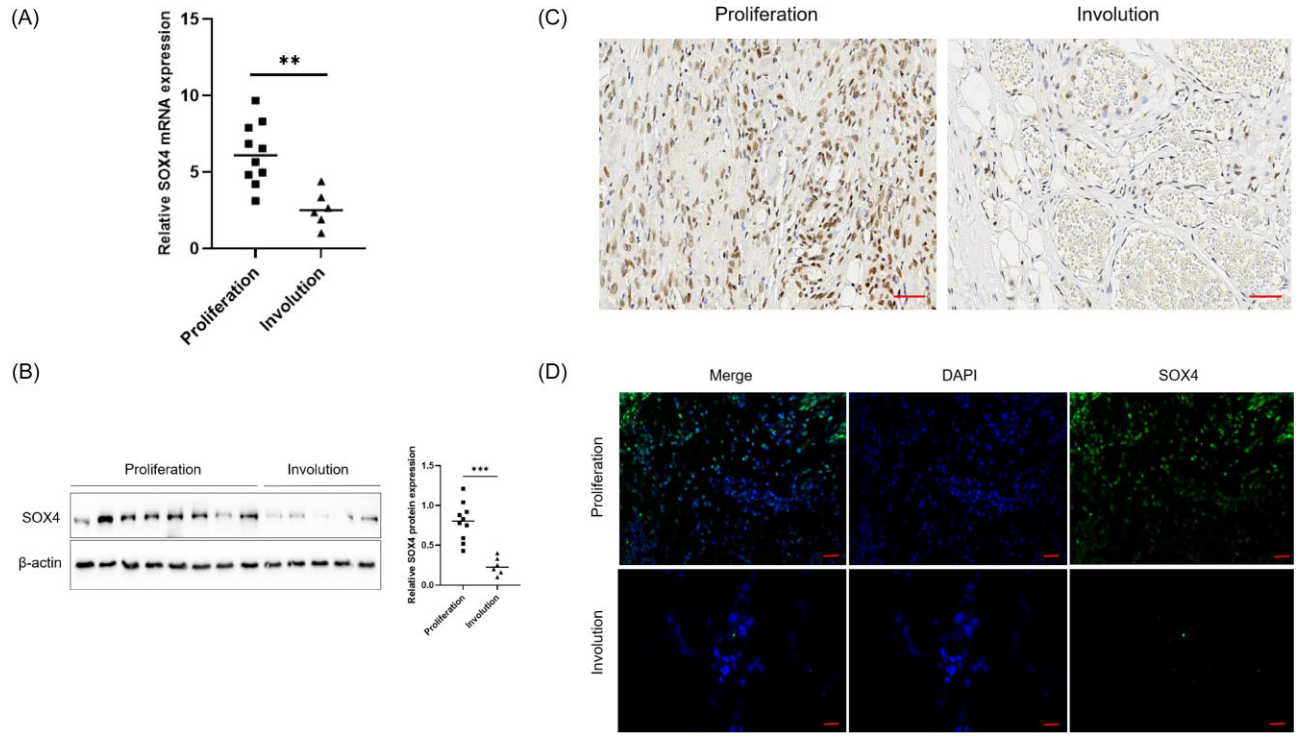

Figure 1. SOX4 was highly expressed in IH tissues during the proliferative phase. (**A**) qRT-PCR results showing that the expression of SOX4 mRNA in proliferating-phase IH tissues ($n = 10$) was significantly greater than that in involuting-phase IH tissues ($n = 6$). The data are presented as the mean ± SD. $^{**}P < 0.01$ by Student's t test. (**B**) Western blot results showing that the expression of the SOX4 protein in proliferating-phase IH tissues ($n = 10$) was significantly greater than that in involuting-phase IH tissues ($n = 6$). The data are presented as the mean ± SD. $^{***}P < 0.001$ by Student's t test. (**C**) The IHC results revealed that the SOX4 protein was expressed mainly in the nucleus, and its positive expression in the proliferating-phase IH tissue was significantly greater than that in the involuting-phase IH tissue. Scale bar = 100 μm. (**D**) Immunofluorescence results showing that the SOX4 protein was expressed mainly in the nucleus and that its positive expression in proliferating-phase IH tissue was significantly greater than that in involuting-phase IH tissue. Scale bar = 100 μm.

RNA-seq and enrichment analysis results of SOX4-knockdown CD31+ HemECs

To further explore the downstream genes and signaling pathways associated with SOX4, we conducted RNA-seq screening of DEGs in CD31+ HemECs with SOX4 knockdown and in the control group. The results revealed 690 DEGs in the SOX4-knockdown group, with 592 genes significantly upregulated and 98 genes significantly downregulated (Fig. S4A–C, see online supplementary material). Gene ontology enrichment analysis revealed that the upregulated genes are involved in the PI3K/AKT signaling pathway, G protein-coupled receptor binding, nervous system development, and autophagosome assembly (Fig. S4D). The downregulated genes were enriched in cell differentiation, mitochondrial depolarization, the PI3K/AKT signaling pathway, and mitochondrial autophagy (Fig. S4E). Kyoto Encyclopedia of Genes and Genomes analysis highlighted pathways such as animal autophagy, mitochondrial autophagy, estrogen signaling, and cell adhesion (Fig. S4G). These findings reveal potential downstream targets and pathways influenced by SOX4 in IH progression.

Database prediction and ChIP-PCR confirmed that ESM1 was the downstream target gene of SOX4

After analyzing the RNA-seq data from the SOX4 knockdown and control groups, we identified the top 10 downregulated genes (*CHRNA5, PPARGC1B, RP11-417L19.4, FAM216B, ACTR3B, DCLK1, AC092835.2, RP11-136L23.2, ESM1, and NDP*) for further investigation (Table S6, see online supplementary material). ESM1 is closely associated with angiogenesis. ESM1, which is secreted by vascular endothelial cells, promotes cell proliferation, differentiation, adhesion, and angiogenesis by inducing inflammatory cytokines and angiogenic factors. Using the JASPAR database, we predicted SOX4 binding sites in the ESM1 promoter region (Fig. S5A, see online supplementary material) and identified a high-scoring site at −248 to −257 bp. qRT-PCR analysis revealed significant enrichment of the ESM1 promoter in chromatin pulled down by the SOX4 antibody compared with that pulled down by the IgG control (Fig. S5B), indicating that SOX4 can directly bind to the ESM1 promoter. Further validation involved transfecting CD31+ HemECs with si-SOX4 and SOX4-overexpressing cells. The qRT-PCR and Western blot results revealed lower ESM1 expression in the si-SOX4 group and higher expression in the SOX4-overexpressing group (Fig. S5C–F). These findings suggest a positive regulatory relationship between SOX4 and ESM1.

ESM1 is highly expressed in proliferating-phase IH tissues and promotes the angiogenesis of CD31+ HemECs

After identifying SOX4 as a transcriptional activator of ESM1, we confirmed higher ESM1 expression in proliferating-phase IH tissues than in involuting-phase tissues through qRT-PCR and Western blot analyses (Fig. 4A and B). Additionally, a strong correlation ($r = 0.7$) between SOX4 and ESM1 mRNA levels was observed in 16 IH tissue samples (Fig. 4C). IHC and immunoflu-

Downloaded from https://academic.oup.com/pcm/article/7/4/pbae026/7816374 by guest on 04 December 2025

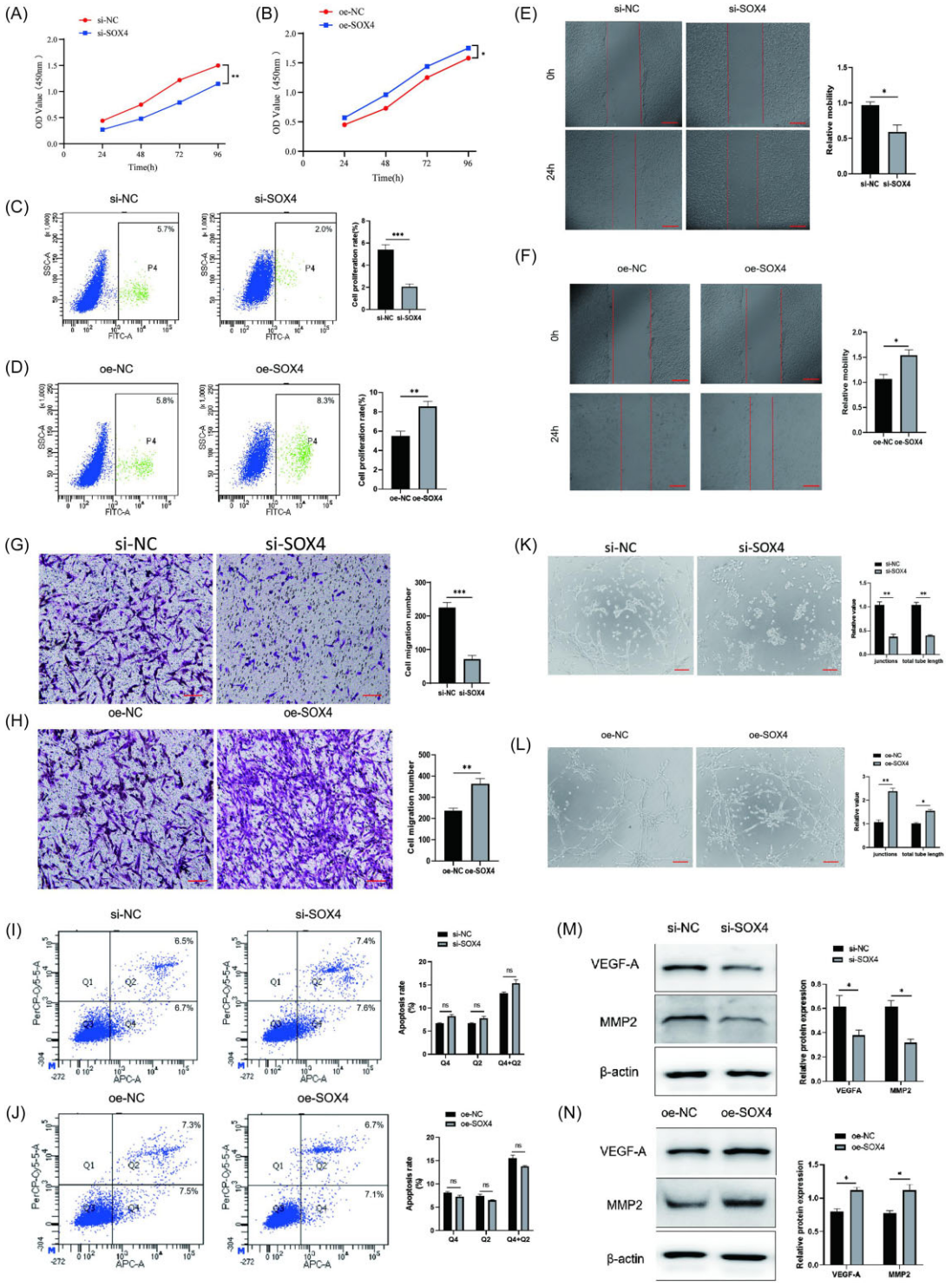

Figure 2. SOX4 promotes angiogenesis and the protein expression of VEGFA and MMP2 in CD31+ HemECs. (**A**) Results of the CCK-8 assay showed that knocking down SOX4 significantly inhibited cell proliferation. (**B**) Results of the CCK-8 assay showed that overexpression of SOX4 significantly promoted cell proliferation. (**C**) EdU results showed that knocking down SOX4 significantly inhibited cell proliferation. (**D**) EdU results showed that overexpression of SOX4 significantly promoted cell proliferation. (**E**) Wound healing assay results showed that SOX4 knockdown significantly inhibited the lateral migration ability of cells. (**F**) Wound healing assay results showed that overexpression of SOX4 significantly promoted the lateral migration of cells. (**G**) Transwell assay results showing that SOX4 knockdown significantly inhibited the longitudinal migration of cells.(**H**) Transwell experiments revealed that SOX4 overexpression significantly promoted the longitudinal migration of CD31+ HemECs. (**I**) Results of the apoptosis experiment revealed that knocking down SOX4 did not significantly promote the apoptosis of CD31+ HemECs. (**J**) Results of the apoptosis experiment revealed that overexpression of SOX4 did not significantly inhibit the apoptosis of CD31+ HemECs. (**K**) Angiogenesis experiments revealed that knocking down SOX4 significantly inhibited the angiogenesis ability of CD31+ HemECs. The figure on the right is a statistical graph of the relative node number and total length of angiogenesis. (**L**) Angiogenesis experiments revealed that the overexpression of SOX4 significantly promoted angiogenesis in CD31+ HemECs. (**M**) Western blot results showing that knocking down SOX4 significantly decreased the protein expression of VEGF-A and MMP2. (**N**) Western blot results showing that knocking down SOX4 significantly increased the protein expression of VEGF-A and MMP2. Data are presented as the mean ± SD ($n = 3$). $^*P < 0.05$, $^{**}P < 0.01$, $^{***}P < 0.001$ by ANOVA; ns, not significant. Scale bars = 100 μm.

Downloaded from https://academic.oup.com/pcm/article/7/4/pbae026/7816374 by guest on 04 December 2025

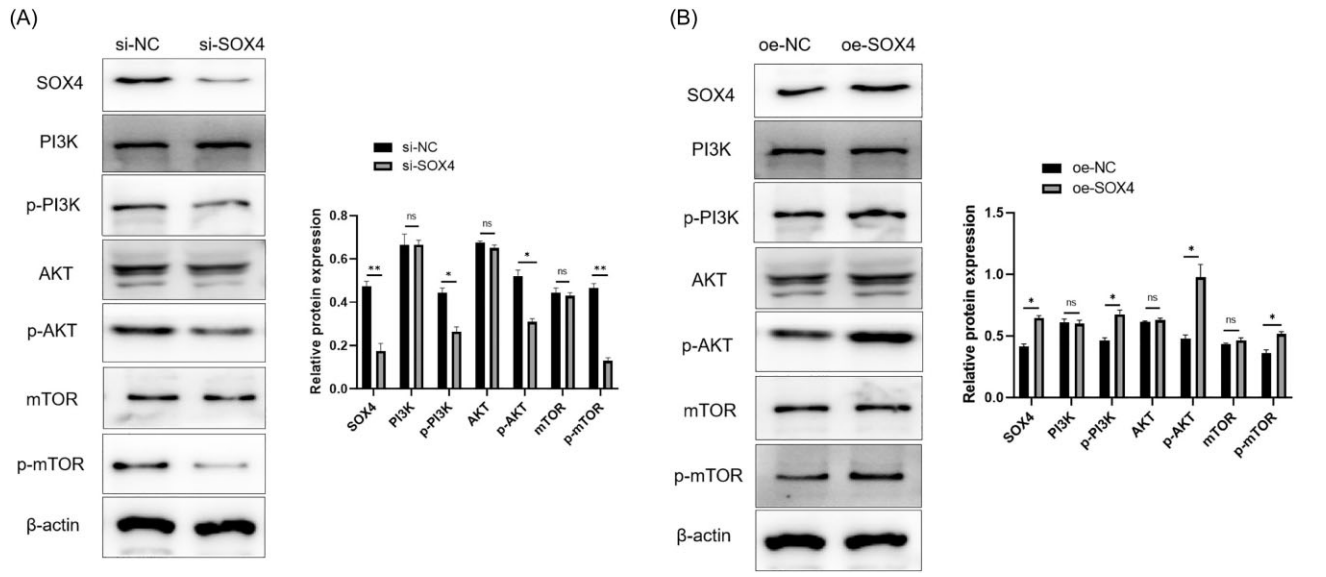

Figure 3. SOX4 may play a role in activating the PI3K/AKT signaling pathway through phosphorylation. (**A**) Potein expression of p-PI3K, p-AKT and p-mTOR was significantly inhibited by SOX4 knockout, but the total protein levels of PI3K, AKT, and mTOR were not significantly affected. (**B**) Overexpression of SOX4 significantly promoted the protein expression of p-PI3K, p-AKT, and p-mTOR but did not significantly change the total protein levels of PI3K, AKT, and mTOR. Data are presented as mean ± SD (n = 3). *$P < 0.05$, **$P < 0.01$ by Student's t test; ns, not significant.

orescence results revealed that the ESM1 protein is expressed mainly in the cytoplasm of IH tissue, with higher expression during the proliferating phase than during the involuting phase (Fig. 4D and E). These findings suggest that ESM1 may play a role in the progression of IH. To further explore the role of ESM1 in IH, we transfected a siRNA targeting ESM1 and an ESM1 overexpression plasmid into CD31+ HemEC cells and successfully established an ESM1 knockdown group and an overexpression group (Fig. S6, see online supplementary material). Functional assays, including CCK-8, EdU, cell scratch, Transwell, and angiogenesis assays, demonstrated that ESM1 knockdown significantly inhibited the proliferation, migration, and angiogenesis of CD31+ HemECs (Figs 5F, and 4J, L, N and P). Conversely, overexpression of ESM1 promoted these biological behaviors in CD31+ HemECs (Fig. 4G, K, M, O and Q). Western blot analysis revealed that ESM1 knockdown suppressed the protein expression of VEGF-A and MMP2 (Fig. 4H), whereas ESM1 overexpression increased their expression (Fig. 4I).

ESM1 may play a role in activating the PI3K/AKT signaling pathway

Through database prediction and ChIP-PCR analysis, we confirmed that ESM1 is a downstream gene directly regulated by SOX4. A literature review highlighted the role of ESM1 in promoting cellular behaviors such as proliferation, migration, invasion, and angiogenesis via the PI3K/AKT pathway, accelerating tumor progression [37]. Thus, we hypothesized that ESM1 is involved in IH development through PI3K/AKT signaling. By manipulating ESM1 expression in CD31+ HemECs, we observed that ESM1 knockout significantly reduced p-PI3K, p-AKT, and p-mTOR protein levels (Fig. 5A), whereas ESM1 overexpression increased these levels (Fig. 5B), implicating ESM1 in IH progression via PI3K/AKT activation.

SOX4-mediated transcriptional activation of ESM1 promotes CD31+ HemEC progression

In previous studies, we demonstrated that SOX4 can transcriptionally activate ESM1, leading to the promotion of angiogenesis in CD31+ HemECs. Given this relationship, can ESM1 function as an effector of SOX4 to enhance the biological behaviors of CD31+ HemECs? To investigate this possibility, we conducted a functional experiment in which ESM1 was simultaneously overexpressed in CD31+ HemEC cells with SOX4 knockdown. We transfected si-SOX4 and si-SOX4+ oe-ESM1 into CD31+ HemECs for 48 h and then conducted a cell behavior recovery experiment. Compared with those in the control group, the proliferation, migration, and angiogenesis of cells in the low SOX4 group were significantly lower (Fig. 6A–E). Furthermore, compared with that in the low SOX4 group, angiogenesis in CD31+ HemECs in the low SOX4+ overexpressing ESM1 group was partially restored (Figs 6A–E). Additionally, Western blot analysis revealed that the expression of VEGF-A, MMP2, and factors related to the PI3K/AKT pathway and vascular endothelial function was significantly lower in the SOX4 knockout group than in the control group (Fig. 6F). However, compared with those in the SOX4-knockdown group, the protein levels of VEGF-A, MMP2, and PI3K/AKT pathway-related factors in the SOX4-overexpressing ESM1-cotransfection group were partially rescued (Fig. 6G).

SOX4-mediated transcriptional activation of ESM1 promotes 3D microtumour proliferation

We will continue to investigate the effect of the SOX4–ESM1 signaling axis on the proliferation ability of CD31+ HemEC 3D microtumors. Ki-67 immunofluorescence staining was performed to further observe the difference in the cell proliferation ability of the microtumors in each group. Compared with those in the negative control group, the proliferation ability of cells in the low SOX4 group was significantly reduced, whereas the proliferation ability of cells in the ESM1 overexpression group was significantly

Downloaded from https://academic.oup.com/pcm/article/7/4/pbae026/7816374 by guest on 04 December 2025

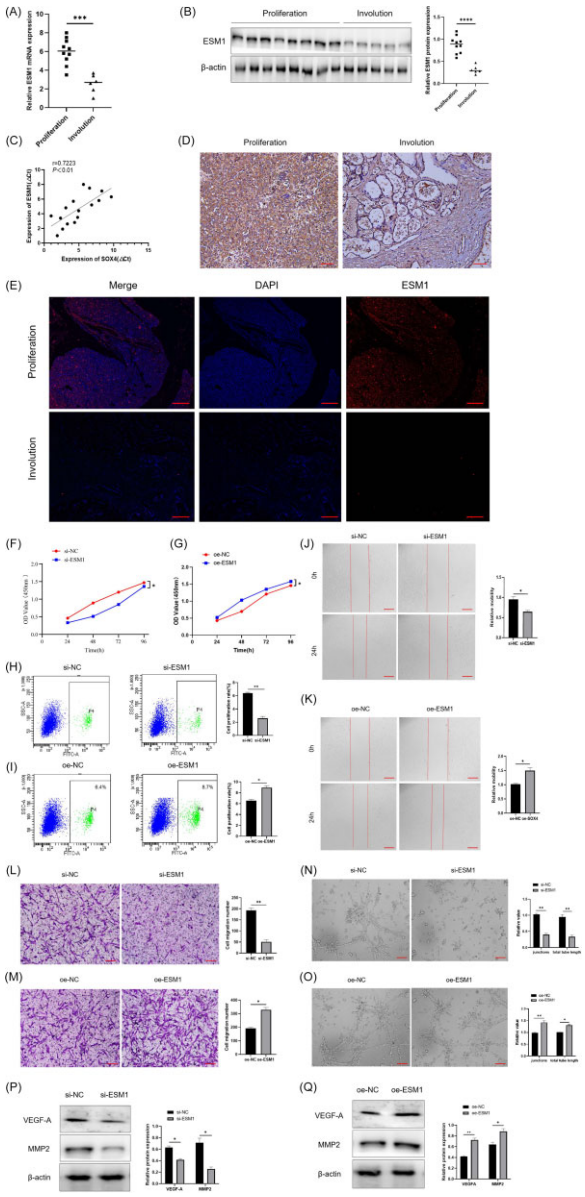

Figure 4. ESM1 was highly expressed in IH tissues during the proliferative phase and promoted CD31+ HemEC angiogenesis and the expression of the VEGFA and MMP2 proteins. (**A**) qRT-PCR results showing that the expression of ESM1 mRNA was significantly greater in the proliferating phase ($n = 10$) than in the involuting phase ($n = 6$). The data are presented as the mean ± SD. ***$P < 0.001$ by Student's t test. (**B**) Western blot results showing that the expression of the ESM1 protein in the proliferating phase ($n = 10$) was significantly greater than that in the involuting phase ($n = 6$). The data are presented as the mean ± SD. ****$P < 0.0001$ by Student's t test. (**C**) There was a positive correlation between SOX4 and ESM1 mRNA in 16 IH tissues ($r = 0.72$, Pearson analysis). (**D**) IHC results revealed that the ESM1 protein was expressed mainly in the cytoplasm, and its positive expression was significantly greater in the proliferating phase than in the involuting phase. Scale bar = 100 μm. (**E**) Immunofluorescence results revealed that the ESM1 protein was expressed mainly in the cytoplasm, and its positive expression in the proliferating phase was significantly greater than that in the involuting phase. Scale bar = 100 μm. (**F**) CCK-8 results showing that the knockdown of ESM1 significantly inhibited cell proliferation. The data are presented as the mean ± SD ($n = 3$). *$P < 0.05$ by ANOVA. (**G**) CCK-8 results showing that the overexpression of ESM1 significantly promoted cell proliferation. The data are presented as the mean ± SD ($n = 3$). *$P < 0.05$ by ANOVA. (**H**) Western blot results showing that knocking down ESM1 significantly decreased the protein expression of VEGF-A and MMP2 in cells. The figure on the right shows the statistical analysis of the relative protein expression levels of VEGF-A and MMP2. The data are presented as the mean ± SD ($n = 3$). **$P < 0.01$ by ANOVA. (**I**) Western blot results showing that overexpression of ESM1 significantly increased the protein expression levels of VEGF-A and MMP2 in cells. The data are presented as the mean ± SD ($n = 3$). *$P < 0.05$ by ANOVA. (**J**) Angiogenesis experiments revealed that ESM1 knockout significantly inhibited angiogenesis. The figure on the right shows the relative number of nodes and total length of tubules in the two groups. The data are presented as the mean ± SD ($n = 3$). *$P < 0.05$ by ANOVA. (**K**) Angiogenesis experiments revealed that the overexpression of ESM1 significantly promoted angiogenesis in cells. The figure on the right shows the relative number of nodes and the total length of tubule formation. The data are presented as the mean ± SD ($n = 3$). *$P < 0.05$ by ANOVA. (**L**) Transwell migration experiments revealed that ESM1 knockdown significantly inhibited the longitudinal migration ability of cells. The data are presented as the mean ± SD ($n = 3$). **$P < 0.01$ by ANOVA. (**M**) Transwell migration experiments revealed that the overexpression of ESM1 significantly promoted the longitudinal migration ability of cells. The figure on the right is a statistical graph of the number of migrating cells. (**N**) EdU results showed that the knockdown of ESM1 significantly inhibited cell proliferation. The data are presented as the mean ± SD ($n = 3$). *$P < 0.05$ by ANOVA. (**O**) EdU results showed that the overexpression of ESM1 significantly promoted cell proliferation. The data are presented as the mean ± SD ($n = 3$). *$P < 0.05$, **$P < 0.01$ by ANOVA. (**P**) Wound healing assay results showed that knocking down ESM1 significantly inhibited the lateral migration ability of cells. The data are presented as the mean ± SD ($n = 3$). *$P < 0.05$ by Student's t test. (**Q**) Wound healing assay results showing that the overexpression of ESM1 significantly promoted the lateral migration ability of cells. The data are presented as the mean ± SD ($n = 3$). *$P < 0.05$, **$P < 0.01$ by Student's t test.

Downloaded from https://academic.oup.com/pcm/article/7/4/pbae026/7816374 by guest on 04 December 2025

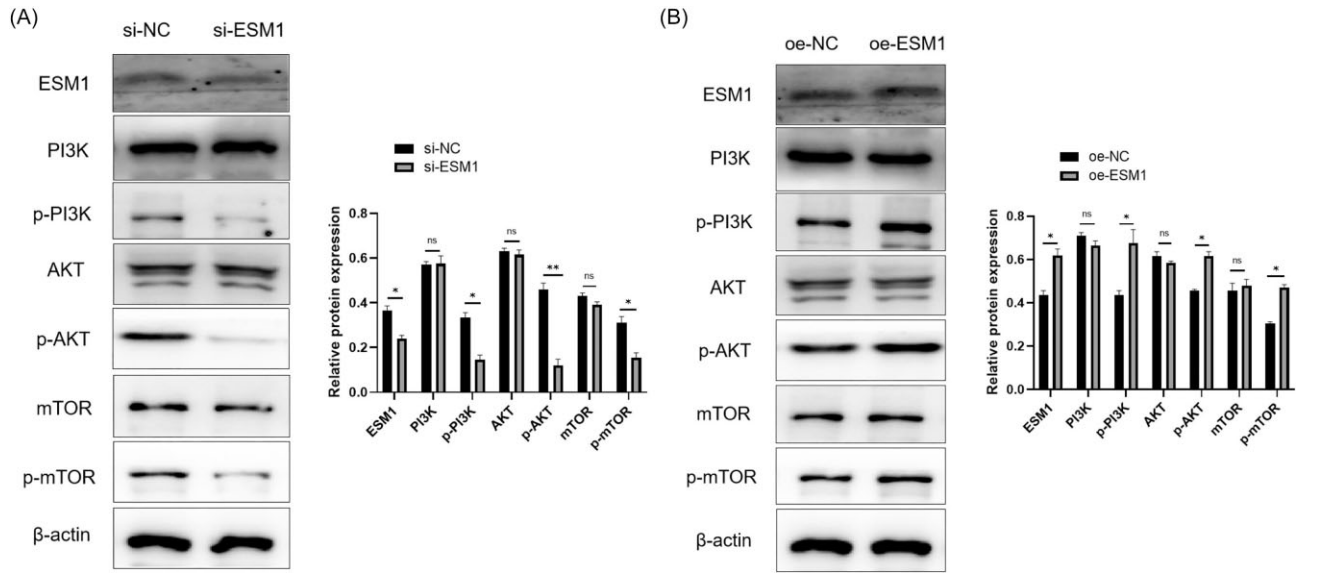

Figure 5. ESM1 may play a role by activating the PI3K/AKT signaling pathway through phosphorylation. (**A**) Knockdown of ESM1 significantly inhibited the protein expression of p-PI3K, p-AKT, and p-mTOR but had no significant effect on the total protein levels of PI3K, AKT, or mTOR. The data are presented as the mean ± SD ($n = 3$). (**B**) Overexpression of ESM1 significantly promoted the protein expression of p-PI3K, p-AKT, and p-mTOR in cells but had no significant effect on the total protein levels of PI3K, AKT, or mTOR. The statistical graph of relative protein expression is shown on the right. Data are presented as mean ± SD ($n = 3$). *$P < 0.05$, **$P < 0.01$ by Student's t test.

enhanced (Fig. 7). Compared with that in the low SOX4 group, the proliferation of cells in the low SOX4+ overexpressing ESM1 cotransfection group was partially restored (Fig. 7). These results indicate that SOX4 can promote the progression of IH by affecting the proliferation of 3D microtumour cells, but this effect can be partially inhibited by ESM1.

Activation of ESM1 by SOX4 transcription promotes IH progression in nude mice

The results of subcutaneous tumor formation in nude mice revealed that, compared with that in the control group, the tumor volume in the low SOX4 group was significantly smaller, whereas the tumor volume in the ESM1 overexpression group was significantly larger (Fig. 8A). Compared with that in the low SOX4 group, the tumor volume in the low SOX4+ overexpressing ESM1 cotransfection group was partially restored (Fig. 8A). HE and CD31 antibody-labeled IHC staining of the tumor tissue from each group was performed to further analyze the differences in the MVD. HE staining revealed that the capillaries in the tumor tissues of the control group were evenly distributed and that the number of capillaries was moderate, whereas the capillaries in the tumor tissues of the SOX4 group were sparsely distributed, the number of capillaries decreased significantly, and interstitial fiber tissue hyperplasia was obvious (Fig. 8B). In the ESM1-overexpressing group, the capillaries were closely arranged, and the number of capillaries increased significantly (Fig. 8B). The density and number of capillaries in the tumors cotransfected with low SOX4+ overexpressing ESM1 were between those in the control group and those in the low SOX4 group (Fig. 8B). The MVD of the tumor tissues further revealed that, compared with that in the control group, the MVD of the tumor tissues was significantly lower in the SOX4 knockout group and significantly greater in the ESM1 overexpression group (Fig. 8C). Compared with that in the low SOX4 group, the MVD of tumors in the low SOX4+ overexpressing ESM1 cotransfection group was reversed to a certain extent (Fig. 8C). According to the study results, SOX4 can promote the progression of tumors in nude mice by affecting cell proliferation and blood vessel formation, but some of its effects can also be inhibited by ESM1.

Discussion

Currently, the pathogenesis of IH is not fully understood. It has been reported that IH may result from the clonal expansion of stem cells due to key gene mutations in somatic cells [40, 41]. Other studies have suggested that tissue hypoxia and the renin–angiotensin system may also be independent and significant risk factors for IH [42–44]. To identify key genes potentially related to IH pathogenesis, we conducted RNA-seq on IH 3D microtumors and 2D planar cells and analyzed the upregulated genes in addition to those from IH tissues in the early proliferating and involuting phases. The results indicated a potential close association between the transcription factor SOX4 and the onset and progression of IH.

SOX4 is a critical developmental transcription factor that regulates cell fate, differentiation, and progenitor cell development. SOX4 is an essential gene in mouse heart development, and complete SOX4 knockout results in embryonic lethality. Additionally, impaired B lymphocyte development has been observed in SOX4-knockout mouse embryos, suggesting a potential link to vascular system development [45]. SOX4 plays diverse roles in different tumors. While it acts as a protumor factor in breast cancer, lung cancer, glioma, and other cancers by promoting cell proliferation, survival, and migration and inhibiting apoptosis [46–49], it inhibits tumor growth in bladder cancer, hepatocellular carcinoma, glioblastoma multiforme, and other cancers [50, 51]. Nevertheless, the literature on the role of SOX4 in IH remains scarce, and relevant mechanistic or functional studies that effectively describe the potential biological functions of SOX4 in IH progression are lacking. We observed significantly greater expression of SOX4 in microtumours than in 2D ordinary cells. Additionally, the expression of

Downloaded from https://academic.oup.com/pcm/article/7/4/pbae026/7816374 by guest on 04 December 2025

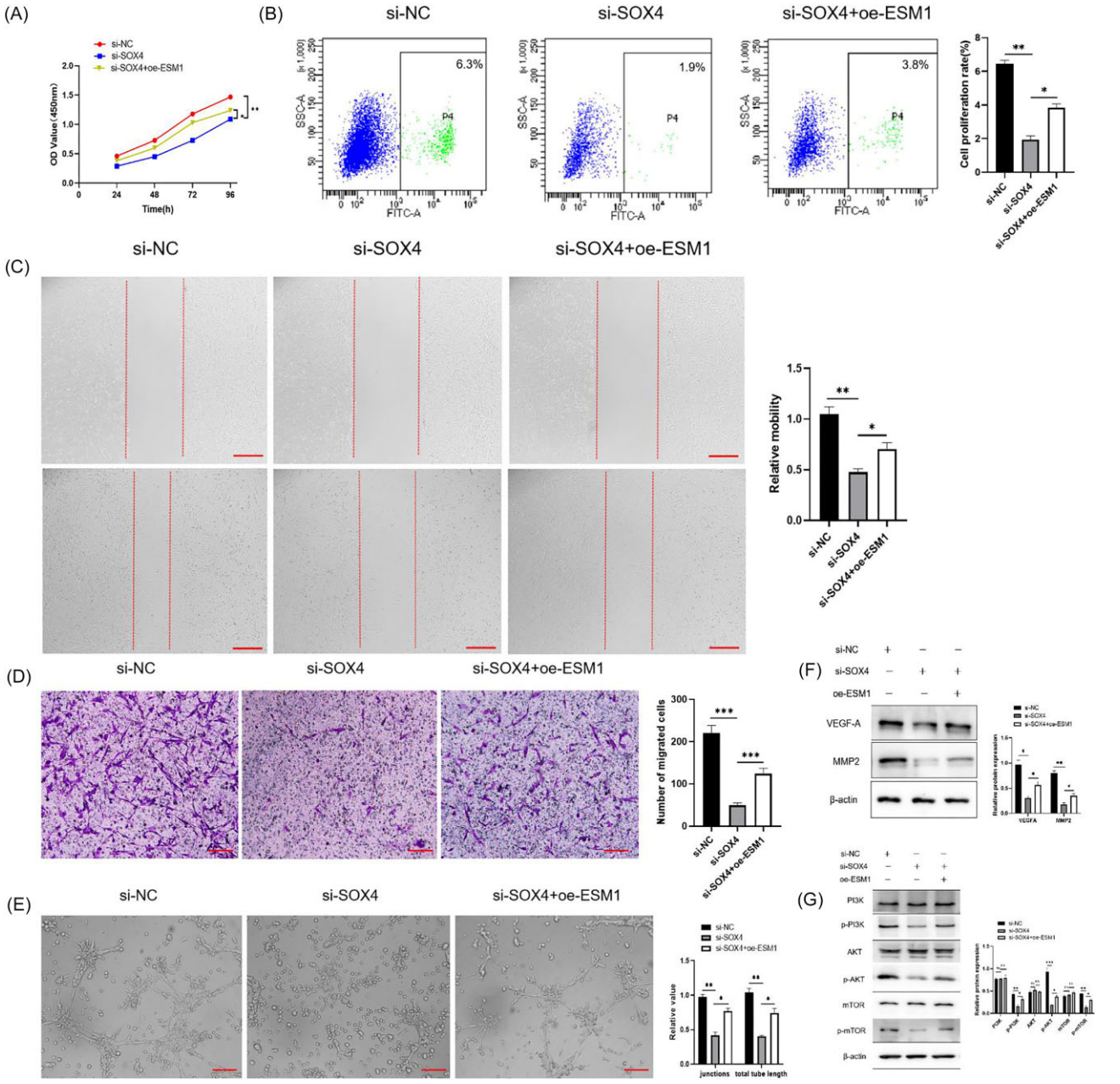

Figure 6. SOX4-mediated transcriptional activation of ESM1 promotes CD31+ HemEC progression. (**A**) CCK-8 results revealed that, compared with the low SOX4 group, knocking down SOX4 while overexpressing ESM1 could partially reverse cell proliferation. (**B**) EdU results showed that the overexpression of ESM1 at the same time as SOX4 knockdown could partially reverse cell proliferation compared with that in the SOX4 knockdown group. (**C**) Wound healing assay revealed that, compared with the low SOX4 group, low SOX4 combined with overexpression of ESM1 could partially reverse the lateral migration ability of the cells. (**D**) Transwell migration results revealed that, compared with that of the low SOX4 group, the vertical migration ability of cells could be partially reversed by low SOX4 and overexpression of ESM1. (**E**) Angiogenesis experiments revealed that, compared with that in the low SOX4 group, low SOX4 combined with overexpression of ESM1 could partially reverse the angiogenesis ability of cells. The figure on the right shows the relative number of nodes and total length of tubule formation. (**F**) Western blot results showing that, compared with those in the SOX4-knockdown group, the protein expression of VEGF-A and MMP2 in cells was partially upregulated by simultaneous overexpression of ESM1 in the SOX4-knockdown group. The figure on the right is a statistical graph of the relative protein expression levels of VEGF-A and MMP2. (**G**) Western blot results showing that, compared with the SOX4 knockout group, the SOX4 knockout combined with ESM1 overexpression group exhibited partial upregulation of p-PI3K, p-AKT, and p-mTOR protein expression in cells. The figure on the right shows the relative expression levels of key proteins in the PI3K/AKT signaling pathway. Data are presented as mean ± SD ($n = 3$). $^{*}P < 0.05$, $^{**}P < 0.01$, $^{***}P < 0.001$ by ANOVA. Scale bars = 100 μm.

SOX4 was significantly greater in proliferating IH tissues than in involuting-phase tissues, suggesting that SOX4 may play a crucial role in the pelletizing process of CD31+ HemECs and the progression of IH. Furthermore, we discovered that SOX4 substantially promotes CD31+ HemEC angiogenesis and other behaviors. In a study by Li *et al.*, differentially expressed epigenetic genes in IH tissues and adjacent normal tissues were analyzed [52], revealing that SOX4 may act as a transcription factor that plays a vital role in the progression of IH. Subsequent research on human umbilical vein endothelial cells suggested that SOX4 could promote IH progression by inhibiting apoptosis and promoting angiogenesis. It is speculated that SOX4 promotes tumor progression through

Downloaded from https://academic.oup.com/pcm/article/7/4/pbae026/7816374 by guest on 04 December 2025

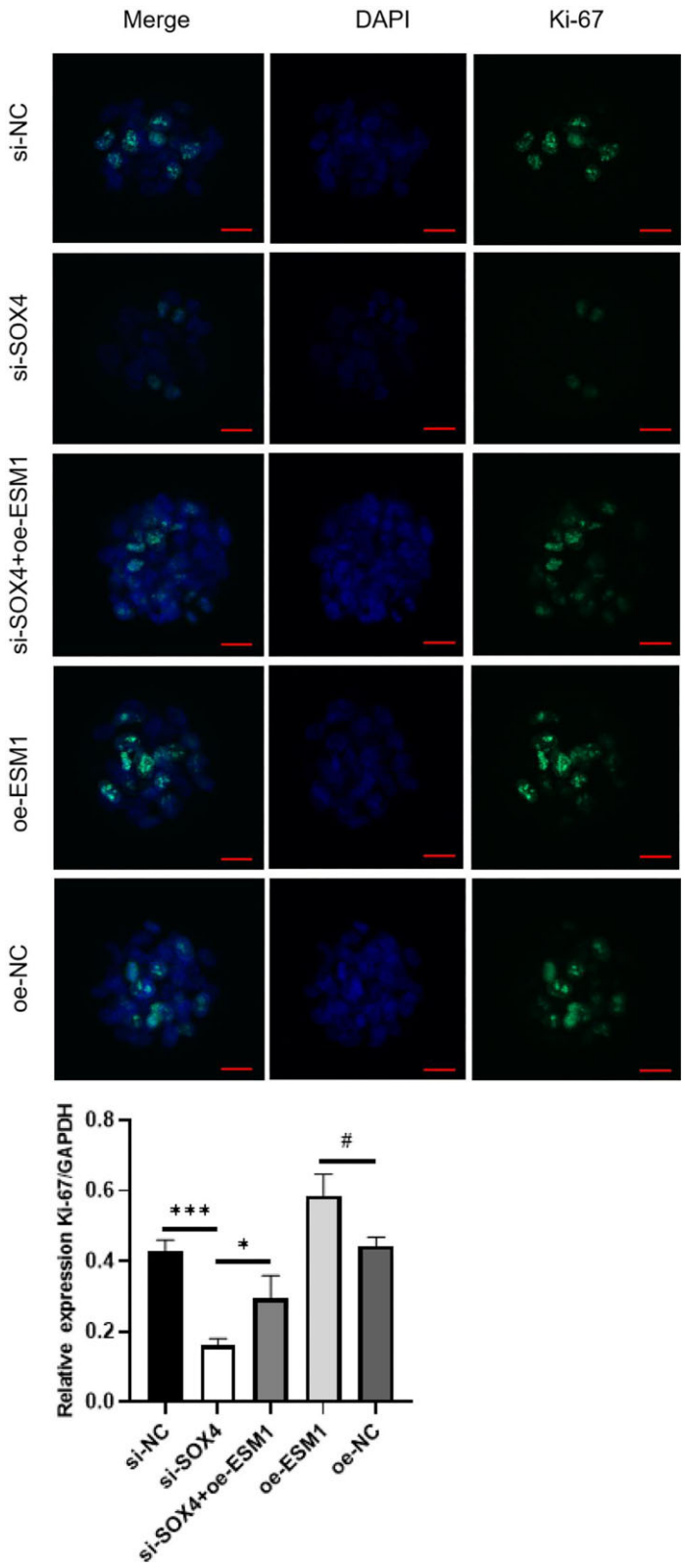

Figure 7. SOX4-mediated transcriptional activation of ESM1 promotes 3D microtumour proliferation in CD31+ HemECs. Ki-67 immunofluorescence staining revealed that, compared with that in the control group, the proliferation ability of cells in the SOX4-knockdown group was significantly decreased, whereas the proliferation ability of cells in the ESM1-overexpressing group was significantly enhanced. Compared with that in the low SOX4 group, the proliferation ability of cells in the low SOX4+ overexpressing ESM1 cotransfection group was partially restored. Data are presented as mean ± SD ($n = 3$). $^{*}P < 0.05$, $^{***}P < 0.001$ by ANOVA. $^{\#}P < 0.05$ by Student's t test. Scale bar = 100 μm.

Downloaded from https://academic.oup.com/pcm/article/7/4/pbae026/7816374 by guest on 04 December 2025

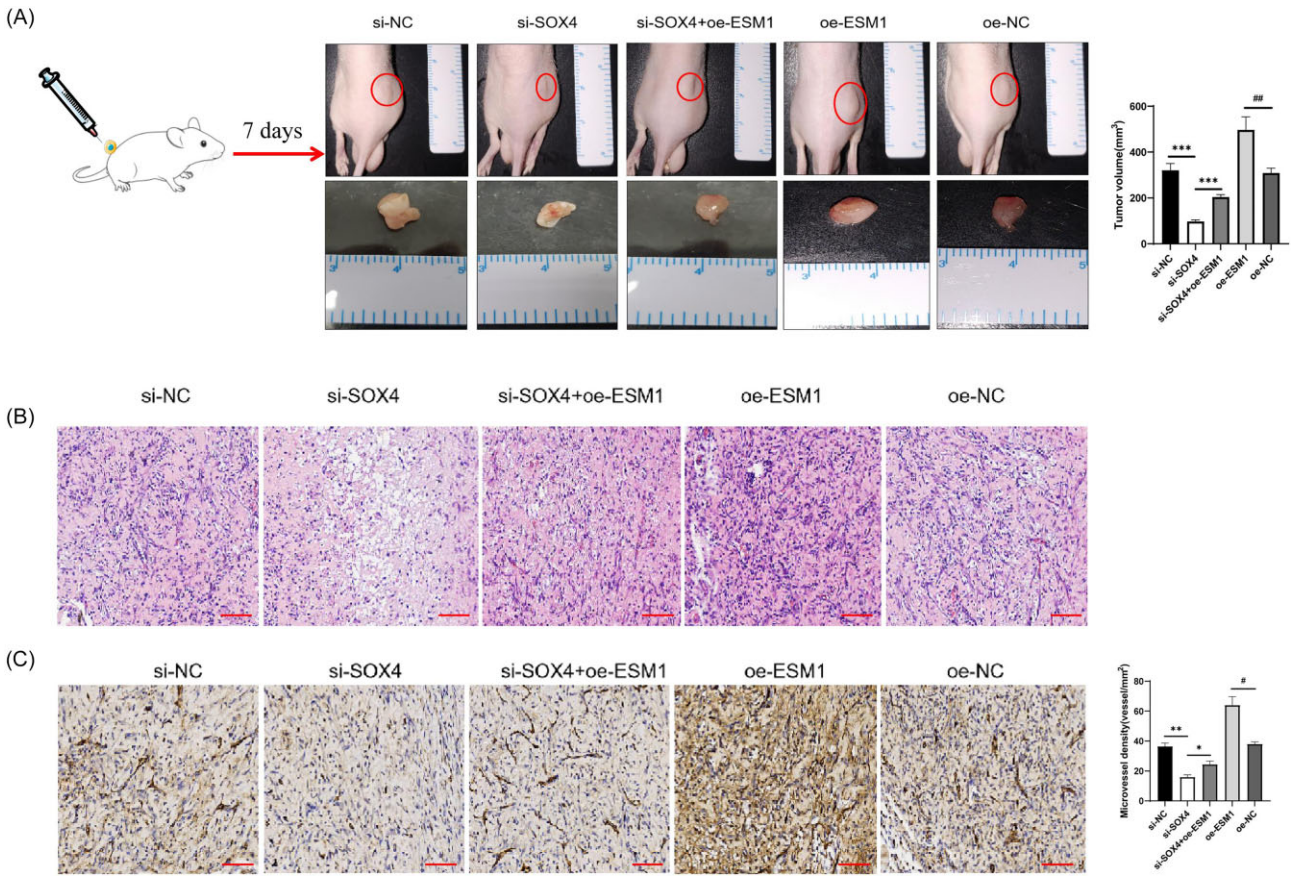

Figure 8. Activation of ESM1 by SOX4 transcription promotes IH progression in nude mice. (**A**) Compared with that of the control group, the tumor volume of the SOX4-knockdown group decreased significantly, whereas the tumor volume of the ESM1-overexpressing group increased significantly. Compared with that of the low SOX4 group, the tumor volume of the low SOX4+ overexpressing ESM1-cotransfected group was partially restored. Data are presented as mean ± SD ($n = 5$). ***$P < 0.001$ by ANOVA; $^{\#\#}P < 0.01$ by Student's t test. (**B**,**C**) The same result was obtained for the MVD. Data are presented as mean ± SD ($n = 5$). *$P < 0.05$, **$P < 0.01$ by ANOVA. Scale bar = 100 μm.

mechanisms such as cell proliferation and survival promotion, apoptosis inhibition, and EMT promotion. These findings align with our results, suggesting that SOX4 may promote IH growth by enhancing cell angiogenesis and other behaviors. Our study is the first to investigate the differential expression of SOX4 between IH microtumours and IH proliferative tissues, suggesting that SOX4 may be a crucial regulatory factor for the rapid growth of IH during the proliferative phase. It could serve as a diagnostic biomarker and therapeutic target for IH in the future. Furthermore, our study revealed that SOX4 significantly upregulated VEGF-A and MMP2 in CD31+ HemECs. Angiogenesis is crucial for the development of IH, and the rapid growth of IH is driven primarily by the proliferation of vascular endothelial cells to form abnormal hemangioma clusters. VEGF-A, the most effective angiogenic factor involved in the progression of IH, may stimulate the proliferation and migration of endothelial cells by activating MMP2, ultimately leading to abnormal angiogenesis [53]. Additionally, VEGF-A may directly promote endothelial cell formation by inducing calcium ion influx through phospholipase C activation. It may also stimulate endothelial cell mitosis and induce blood vessel formation.

Recent studies have confirmed the significant involvement of the PI3K/AKT signaling pathway in the occurrence and development of IH [54, 55]. In our study, we discovered that SOX4 can promote the expression of key proteins within the PI3K/AKT signaling pathway, thereby facilitating the progression of IH. Notably, Mehta *et al*. reported that amplification of the SOX4 gene promotes the PI3K/AKT signaling pathway in breast cancer, highlighting its potential as a therapeutic target and biomarker within this signaling pathway [56]. Similarly, other studies have revealed that SOX4 regulates the PI3K/AKT signaling pathway to promote the progression of acute lymphoblastic leukemia, pancreatic cancer, and colon cancer via transcriptional activation of LEMD1 [57–59]. These findings align with our observations, which demonstrate for the first time that SOX4 can contribute to the progression of IH by activating the PI3K/AKT signaling pathway. However, the precise mechanism through which SOX4 regulates this pathway remains unclear. We hypothesize that the transcription factor SOX4 may activate the PI3K/AKT signaling pathway in cells by binding to key downstream target genes, thereby promoting the development of IH.

ESM1 is secreted by vascular endothelial cells and is involved primarily in angiogenesis, cell adhesion, and the inflammatory response. Numerous studies have reported a close association between ESM1 and angiogenesis, suggesting its involvement in the progression of various malignant tumors [60]. In hepatocellular carcinoma, ESM1 significantly enhances tumor angiogenesis, particularly in the early stages [61]. Studies on breast cancer have demonstrated that ESM1 can activate the AKT/NF-κB signaling pathway to promote cell proliferation, migration, and invasion [62]. Similarly, in esophageal cancer, ESM1 acts as an independent prognostic factor and promotes cell proliferation and migration through the JAK signaling pathway; silencing ESM1

Downloaded from https://academic.oup.com/pcm/article/7/4/pbae026/7816374 by guest on 04 December 2025

significantly inhibits tumor cell proliferation and migration [63]. Additionally, ESM1 is highly expressed in head and neck squamous cell carcinoma and may contribute to tumor progression through the RAS–MAPK–ERK signaling pathway [64]. Thus, ESM1 may promote the progression of malignant tumors by enhancing angiogenesis. In our study, by conducting RNA-seq on SOX4-knockdown CD31+ HemECs, we discovered that ESM1 may be downstream of SOX4 transcriptional regulation. This finding was further confirmed by database prediction and ChIP-PCR, which confirmed the direct regulatory relationship between SOX4 and the ESM1 promoter region. We subsequently examined the impact of ESM1 regulation alone on the biological behavior of CD31+ HemECs. Our studies revealed that ESM1 enhances cell angiogenesis, thereby promoting the progression of IH. These findings align with previous reports, indicating that ESM1 promotes the occurrence and development of IH through cell angiogenesis. Moreover, ESM1 could be explored as a potential therapeutic target for IH. Furthermore, we observed that ESM1 promotes the activation of the PI3K/AKT signaling pathway, thereby contributing to the progression of IH. Similar observations have been reported in cervical cancer, where ESM1 activates the PI3K/AKT signaling pathway and EMT, leading to increased proliferation, migration, and invasion of cancer cells [65]. Additionally, a recent study by Yang *et al*. revealed that ESM1 induces angiogenesis in colorectal cancer by activating the PI3K/AKT/mTOR pathway, thus accelerating tumor progression [66]. These studies support our findings and suggest that ESM1 also promotes the development of IH by activating the PI3K/AKT signaling pathway.

Microtumour and subcutaneous tumor formation experiments in nude mice revealed that low SOX4 expression alone inhibited tumor growth, that overexpression of ESM1 promoted tumor growth, and that simultaneous overexpression of ESM1 and low SOX4 partially restored tumor growth. Therefore, ESM1 can be considered a new therapeutic target for IH. ESM1 has been reported to be associated with drug resistance [67]. In patients with prolactinoma, ESM1 microvascular density was significantly greater in bromocriptine-resistant patients than in bromocriptine-sensitive patients. Knockdown of ESM1 with interfering RNA significantly increased the sensitivity of rat prolactinoma cell lines to dopamine agonists. Additionally, ESM1 knockdown significantly increased the sensitivity of human umbilical vein endothelial cells to bevacizumab [68]. Thus, ESM1 has potential for further study as a target for propranolol treatment in patients with drug-resistant IH. Recent studies have also linked ESM1 to angiogenesis. Research on the mechanism of angiogenesis has revealed a positive feedback loop between VEGF-A and ESM1, where VEGF-A stimulates ESM1 expression through phosphorylation and activation of vascular epidermal growth factor receptor 2 [69]. Conversely, ESM1 directly binds to fibronectin, replacing fibronectin-bound VEGF-A, thereby increasing the bioavailability of VEGF-A and its mediated signaling [70]. Therefore, blocking the interaction between ESM1 and VEGF-A is expected to become a new strategy for inhibiting angiogenesis, and targeted inhibition of ESM1 may control the progression of IH in the future.

However, there are limitations to this study. First, the clinical data and tissue samples were obtained from a single center, and the sample size was relatively small. In the next phase, collaboration with multiple centers will be pursued to establish a clinical sample database and expand the number of samples to increase the accuracy of the results. Second, this study did not investigate the effects of drugs (inhibitors) related to the SOX4–ESM1 signaling axis on IH progression, which will be the focus of our future research. These findings offer a new perspective on the occurrence and development of IH and lay the foundation for future treatment strategies. In terms of treatment strategies, interventions targeting the SOX4–ESM1 axis may provide new therapeutic options for clinical practice. By regulating the activity of this axis, it may be possible to effectively inhibit the growth and spread of hemangiomas, thereby improving the prognosis of patients. Therefore, future research should focus on exploring targeted therapeutic methods for this axis and evaluating their effectiveness and safety in clinical practice. This not only helps optimize existing treatment methods but may also provide insights for other types of vascular anomalies. Additionally, the integration of new technologies such as gene editing and bioprinting may offer new ideas and tools for targeted therapy of the SOX4–ESM1 axis [71].

Conclusions

In conclusion, SOX4 plays a crucial role in the initiation and progression of IH, and SOX4/ESM1 may serve as novel biomarkers and potential therapeutic targets for IH, providing a new approach for the future management and treatment of IH.

Abbreviations

IH, Infantile hemangioma; HemECs, hemangioma endothelial cells; ESM1, endothelial cell-specific molecule 1; FBS: fetal bovine serum; VEGF-A, vascular endothelial growth factor A; HCM, extracellular matrix; EMT, epithelial–mesenchymal transition; HE, hematoxylin–eosin; IHC, immunohistochemistry; ChIP-seq, chromatin immunoprecipitation sequencing; MMP2, matrix metalloproteinase 2; MVD, microvessel density; SD, standard deviation; ANOVA, analysis of variance; DEGs, differentially expressed genes.

Acknowledgments

This work was supported by the National Natural Science Foundation of China (Grants No. 82473553 and 82273556), the Key Project in the Science & Technology Program of Sichuan Province (Grants No. 2022YFS0233 and 2022YFS0225), the Postdoctoral Foundation of West China Hospital of Sichuan University (Grant No. 2023HXBH056), the Project of Natural Science Foundation of Shandong Province (Grant No. ZR2022MH229), the '0 to 1' Project of Sichuan University (Grant No. 2022SCUH0033), the Med-X Center for Informatics Funding Project (Grant No. YGJC004), the 1·3·5 Project for Disciplines of Excellence-Clinical Research Incubation Project of West China Hospital of Sichuan University (Grants No. 2023HXFH004, 2020HXFH048 and 2019HXFH056), and the 1·3·5 Project for Disciplines of Excellence-Clinical Research Interdisciplinary Innovation Project of West China Hospital of Sichuan University (Grant No. ZYJC21060). We thank Li Li and Chunjuan Bao (Institute of Clinical Pathology, West China Hospital, Sichuan University) for performing the histological staining.

Author contributions

Yanan Li (Data curation, Formal analysis, Investigation, Methodology, Software), Meng Kong (Conceptualization, Data curation, Methodology, Writing—original draft), Tong Qiu (Data curation), and Yi Ji (Funding acquisition, Methodology, Supervision, Writing—review & editing).

Downloaded from https://academic.oup.com/pcm/article/7/4/pbae026/7816374 by guest on 04 December 2025

Supplementary data

Supplementary data is available at *PCMEDI* Journal online.

Conflict of interest

None declared.

Ethics approval and consent to participate

The study was approved by the West China Hospital of Sichuan University Biomedical Research Ethics Committee (No. 2017–414), and informed consent was obtained from all participants or legal guardians.

Data availability

All relevant data are contained within the article. The original contributions presented in the study are included in the supplementary material. Additional data supporting the findings of this article are available from the corresponding author upon reasonable request.

References

1. Mariani LG, Ferreira LM, Rovaris DL *et al.* Infantile hemangiomas: risk factors for complications, recurrence and unaesthetic sequelae. *An Bras Dermatol* 2022;**97**:37–44. https://doi.org/10.1016/j.abd.2021.05.009.
2. Tan X, Guo S, Wang C. Propranolol in the Treatment of Infantile Hemangiomas. *Clin Cosmet Investig Dermatol* 2021;**14**:1155–63. https://doi.org/10.2147/CCID.S332625.
3. Anderson KR, Schoch JJ, Lohse CM *et al.* Increasing incidence of infantile hemangiomas (IH) over the past 35 years: Correlation with decreasing gestational age at birth and birth weight. *J Am Acad Dermatol* 2016;**74**:120–6. https://doi.org/10.1016/j.jaad.2015.08.024.
4. Rodríguez Bandera AI, Sebaratnam DF, Wargon O *et al.* Infantile hemangioma. Part 1: Epidemiology, pathogenesis, clinical presentation and assessment. *J Am Acad Dermatol* 2021;**85**:1379–92. https://doi.org/10.1016/j.jaad.2021.08.019.
5. Ji Y, Yang K, Zhou J *et al.* Propranolol for the treatment of ulcerated infantile hemangiomas: A prospective study. *J Am Acad Dermatol* 2022;**86**:1149–51. https://doi.org/10.1016/j.jaad.2021.04.055.
6. Xu W, Li S, Yu F *et al.* Role of Thrombospondin-1 and Nuclear Factor-κB Signaling Pathways in Antiangiogenesis of Infantile Hemangioma. *Plast Reconstr Surg* 2018;**142**:310e–21e. https://doi.org/10.1097/PRS.0000000000004684.
7. Kong M, Li Y, Wang K *et al.* Infantile hemangioma models: is the needle in a haystack? *J Transl Med* 2023;**21**:308. https://doi.org/10.1186/s12967-023-04144-0.
8. Soliman YS, Khachemoune A. Infantile hemangiomas: our current understanding and treatment options. *Dermatol Online J* 2018;**24**:13030. https://doi.org/10.5070/D3249041401.
9. Yang K, Qiu T, Gong X *et al.* Integrated nontargeted and targeted metabolomics analyses amino acids metabolism in infantile hemangioma. *Front Oncol* 2023;**13**:1132344. https://doi.org/10.3389/fonc.2023.1132344.
10. Ji Y, Chen S, Yang K *et al.* Efficacy and Safety of Propranolol vs Atenolol in Infants With Problematic Infantile Hemangiomas: A Randomized Clinical Trial. *JAMA Otolaryngol Head Neck Surg* 2021;**147**:599–607. https://doi.org/10.1001/jamaoto.2021.0454.
11. Schoch JJ, Hunjan MK, Anderson KR *et al.* Temporal trends in prenatal risk factors for the development of infantile hemangiomas. *Pediatr Dermatol* 2018;**35**:787–91. https://doi.org/10.1111/pde.13659.
12. Wang C, Li Y, Xiang B *et al.* Quality of life in children with infantile hemangioma: a case control study. *Health Qual Life Outcomes* 2017;**15**:221. https://doi.org/10.1186/s12955-017-0772-z.
13. Khan ZA, Boscolo E, Picard A *et al.* Multipotential stem cells recapitulate human infantile hemangioma in immunodeficient mice. *J Clin Invest* 2008;**118**:2592–9. https://doi.org/10.1172/JCI33493.
14. Li Y, Zhu X, Kong M *et al.* Three-Dimensional Microtumor Formation of Infantile Hemangioma-Derived Endothelial Cells for Mechanistic Exploration and Drug Screening. *Pharmaceuticals (Basel)* 2022;**15**:1393. https://doi.org/10.3390/ph15111393.
15. Yang K, Li X, Qiu T *et al.* Effects of propranolol on glucose metabolism in hemangioma-derived endothelial cells. *Biochem Pharmacol* 2023;**218**:115922. https://doi.org/10.1016/j.bcp.2023.115922.
16. Liu Y, Zeng S, Jiang X *et al.* SOX4 induces tumor invasion by targeting EMT-related pathway in prostate cancer. *Tumor Biol* 2017;**39**:1010428317694539. https://doi.org/10.1177/1010428317694539.
17. Blancato J, Singh B, Liu A *et al.* Correlation of amplification and overexpression of the c-myc oncogene in high-grade breast cancer: FISH, in situ hybridization and immunohistochemical analyses. *Br J Cancer* 2004;**90**:1612–9. https://doi.org/10.1038/sj.bjc.6601703.
18. Huang P, Deng W, Bao H *et al.* SOX4 facilitates PGR protein stability and FOXO1 expression conducive for human endometrial decidualization. *eLife* 2022;**11**:e72073. https://doi.org/10.7554/eLife.72073.
19. Hanieh H, Ahmed EA, Vishnubalaji R *et al.* SOX4: Epigenetic regulation and role in tumorigenesis. *Semin Cancer Biol* 2020;**67**:91–104. https://doi.org/10.1016/j.semcancer.2019.06.022.
20. Tsai CN, Yu SC, Lee CW *et al.* SOX4 activates CXCL12 in hepatocellular carcinoma cells to modulate endothelial cell migration and angiogenesis in vivo. *Oncogene* 2020;**39**:4695–710. https://doi.org/10.1038/s41388-020-1319-z.
21. Bagati A, Kumar S, Jiang P *et al.* Integrin $\alpha v\beta 6$-TGFβ-SOX4 Pathway Drives Immune Evasion in Triple-Negative Breast Cancer. *Cancer Cell* 2021;**39**:54–67.e9. https://doi.org/10.1016/j.ccell.2020.12.001.
22. Wang H, Huo X, Yang XR *et al.* STAT3-mediated upregulation of lncRNA HOXD-AS1 as a ceRNA facilitates liver cancer metastasis by regulating SOX4. *Mol Cancer* 2017;**16**:136. https://doi.org/10.1186/s12943-017-0680-1.
23. Bellmunt J. Stem-Like Signature Predicting Disease Progression in Early Stage Bladder Cancer. The Role of E2F3 and SOX4. *Biomedicines* 2018;**6**:85. https://doi.org/10.3390/biomedicines6030085.
24. Xu G, Meng Y, Wang L *et al.* miRNA-214-5p inhibits prostate cancer cell proliferation by targeting SOX4. *World J Surg Oncol* 2021;**19**:338. https://doi.org/10.1186/s12957-021-02449-2.
25. Moreno CS. SOX4: The unappreciated oncogene. *Semin Cancer Biol* 2020;**67**:57–64. https://doi.org/10.1016/j.semcancer.2019.08.027.
26. Yang Q, Liang Y, Shi Y *et al.* The ALKBH5/SOX4 axis promotes liver cancer stem cell properties via activating the SHH signaling pathway. *J Cancer Res Clin Oncol* 2023;**149**:15499–510. https://doi.org/10.1007/s00432-023-05309-6.
27. Tian D, Luo L, Wang T. ,*et al.* MiR-296-3p inhibits cell proliferation by the SOX4-Wnt/βcatenin pathway in triple-negative

Downloaded from https://academic.oup.com/pcm/article/7/4/pbae026/7816374 by guest on 04 December 2025

breast cancer. *J Biosci* 2021;**46**:98. https://doi.org/10.1007/s12038-021-00219-6.
28. Kang Y, Lv R, Feng Z *et al.* Tumor-associated macrophages improve hypoxia-induced endoplasmic reticulum stress response in colorectal cancer cells by regulating TGF-β1/SOX4. *Cell Signal* 2022;**99**:110430. https://doi.org/10.1016/j.cellsig.2022.110430.
29. Yang K, Qiu T, Zhou J *et al.* Blockage of glycolysis by targeting PFKFB3 suppresses the development of infantile hemangioma. *J Transl Med* 2023;**21**:85. https://doi.org/10.1186/s12967-023-03932-y.
30. Wang S, Ren L, Shen G *et al.* The knockdown of MALAT1 inhibits the proliferation, invasion and migration of hemangioma endothelial cells by regulating MiR-206/VEGFA axis. *Mol Cell Probes* 2020;**51**:101540. https://doi.org/10.1016/j.mcp.2020.101540.
31. Zhu X, Li Y, Long H *et al.* Tissue-specific micropattern array chips fabricated via decellularized ECM for 3D cell culture. *MethodsX* 2023;**11**:102463. https://doi.org/10.1016/j.mex.2023.102463.
32. Lv Y, Xie X, Zou G *et al.* miR-181b-5p/SOCS2/JAK2/STAT5 axis facilitates the metastasis of hepatoblastoma. *Precis Clin Med* 2023;**6**:pbad027. https://doi.org/10.1093/pcmedi/pbad027.
33. Lv Y, Xie X, Zou G *et al.* SOCS2 inhibits hepatoblastoma metastasis via downregulation of the JAK2/STAT5 signaling pathway. *Sci Rep* 2023;**13**:21814. https://doi.org/10.1038/s41598-023-48591-7.
34. Dong X, He Y, An J *et al.* Increased apoptosis of gingival epithelium is associated with impaired autophagic flux in medication-related osteonecrosis of the jaw. *Autophagy* 2023;**19**:2899–911. https://doi.org/10.1080/15548627.2023.2234228.
35. Ren R, Ding S, Ma K *et al.* Sumoylation fine-tunes endothelial HEY1 in the regulation of angiogenesis. *Circ Res* 2024;**134**:203–22. https://doi.org/10.1161/CIRCRESAHA.123.323398.
36. Zhu F, Jing D, Zhou H *et al.* Blockade of Syk modulates neutrophil immune-responses via the mTOR/RUBCNL-dependent autophagy pathway to alleviate intestinal inflammation in ulcerative colitis. *Precis Clin Med* 2023;**6**:pbad025. https://doi.org/10.1093/pcmedi/pbad025.
37. Castro-Mondragon JA, Riudavets-Puig R, Rauluseviciute I *et al.* JASPAR 2022: the 9th release of the open-access database of transcription factor binding profiles. *Nucleic Acids Res* 2022;**50**:D165–73. https://doi.org/10.1093/nar/gkab1113.
38. Xing Z, Du M, Zhen Y *et al.* LETMD1, a target of KLF4, hinders endothelial inflammation and pyroptosis: A protective mechanism in the pathogenesis of atherosclerosis. *Cell Signal* 2023;**112**:110907. https://doi.org/10.1016/j.cellsig.2023.110907.
39. Yang K, Zhang X, Chen L *et al.* Microarray expression profile of mRNAs and long noncoding RNAs and the potential role of PFK-1 in infantile hemangioma. *Cell Div* 2021;**16**:1. https://doi.org/10.1186/s13008-020-00069-y.
40. Smith CJF, Friedlander SF, Guma M *et al.* Infantile Hemangiomas: An Updated Review on Risk Factors, Pathogenesis, and Treatment. *Birth Defects Res* 2017;**109**:809–15. https://doi.org/10.1002/bdr2.1023.
41. Sun Y, Qiu F, Hu C *et al.* Hemangioma Endothelial Cells and Hemangioma Stem Cells in Infantile Hemangioma. *Ann Plast Surg* 2022;**88**:244–9. https://doi.org/10.1097/SAP.0000000000002835.
42. Wu Y, Yang X, Zhai M *et al.* Real-time optical imaging of the hypoxic status in hemangioma endothelial cells during propranolol therapy. *Front Oncol* 2022;**12**:995745. https://doi.org/10.3389/fonc.2022.995745.
43. Gong X, Li Y, Yang K *et al.* Infantile hepatic hemangiomas: looking backwards and forwards. *Precis Clin Med* 2022;**5**:pbac006. https://doi.org/10.1093/pcmedi/pbac006.
44. Gong X, Qiu T, Feng L *et al.* Maternal and Perinatal Risk Factors for Infantile Hemangioma: A Matched Case–Control Study with a Large Sample Size. *Dermatol Ther (Heidelb)* 2022;**12**:1659–70. https://doi.org/10.1007/s13555-022-00756-4.
45. Schilham MW, Oosterwegel MA, Moerer P *et al.* Defects in cardiac outflow tract formation and pro-B-lymphocyte expansion in mice lacking Sox-4. *Nature* 1996;**380**:711–4. https://doi.org/10.1038/380711a0.
46. Zhang J, Liang Q, Lei Y *et al.* SOX4 induces epithelial–mesenchymal transition and contributes to breast cancer progression. *Cancer Res* 2012;**72**:4597–608. https://doi.org/10.1158/0008-5472.CAN-12-1045.
47. Wang D, Hao T, Pan Y *et al.* Increased expression of SOX4 is a biomarker for malignant status and poor prognosis in patients with non-small cell lung cancer. *Mol Cell Biochem* 2015;**402**:75–82. https://doi.org/10.1007/s11010-014-2315-9.
48. Ikushima H, Todo T, Ino Y *et al.* Autocrine TGF-beta signaling maintains tumorigenicity of glioma-initiating cells through Sry-related HMG-box factors. *Cell Stem Cell* 2009;**5**:504–14. https://doi.org/10.1016/j.stem.2009.08.018.
49. Vervoort SJ, van Boxtel R, Coffer PJ. The role of SRY-related HMG box transcription factor 4 (SOX4) in tumorigenesis and metastasis: friend or foe? *Oncogene* 2013;**32**:3397–409. https://doi.org/10.1038/onc.2012.506.
50. Aaboe M, Birkenkamp-Demtroder K, Wiuf C *et al.* SOX4 expression in bladder carcinoma: clinical aspects and in vitro functional characterization. *Cancer Res* 2006;**66**:3434–42. https://doi.org/10.1158/0008-5472.CAN-05-3456.
51. Zhang J, Jiang H, Shao J *et al.* SOX4 inhibits GBM cell growth and induces G0/G1 cell cycle arrest through Akt-p53 axis. *BMC Neurol* 2014;**14**:207. https://doi.org/10.1186/s12883-014-0207-y.
52. Li X, Chen Y, Fu C *et al.* Characterization of epigenetic and transcriptional landscape in infantile hemangiomas with ATAC-seq and RNA-seq. *Epigenomics* 2020;**12**:893–905. https://doi.org/10.2217/epi-2020-0060.
53. Ji Y, Chen S, Li K *et al.* Signaling pathways in the development of infantile hemangioma. *J Hematol Oncol* 2014;**7**:13. https://doi.org/10.1186/1756-8722-7-13.
54. Ke C, Chen C, Yang M *et al.* Inhibition of infantile hemangioma growth and promotion of apoptosis via VEGF/PI3K/Akt axis by 755-nm long-pulse alexandrite laser. *Biomed J* 2023;**47**:100675. https://doi.org/10.1016/j.bj.2023.100675.
55. Pan WK, Li P, Guo ZT *et al.* Propranolol induces regression of hemangioma cells via the down-regulation of the PI3K/Akt/eNOS/VEGF pathway. *Pediatr Blood Cancer* 2015;**62**:1414–20. https://doi.org/10.1002/pbc.25453.
56. Mehta GA, Parker JS, Silva GO *et al.* Amplification of SOX4 promotes PI3K/Akt signaling in human breast cancer. *Breast Cancer Res Treat* 2017;**162**:439–50. https://doi.org/10.1007/s10549-017-4139-2.
57. Ramezani-Rad P, Geng H, Hurtz C *et al.* SOX4 enables oncogenic survival signals in acute lymphoblastic leukemia. *Blood* 2013;**121**:148–55. https://doi.org/10.1182/blood-2012-05-428938.
58. Xu X, Zong K, Wang X *et al.* miR-30d suppresses proliferation and invasiveness of pancreatic cancer by targeting the SOX4/PI3K-AKT axis and predicts poor outcome. *Cell Death Dis* 2021;**12**:350. https://doi.org/10.1038/s41419-021-03576-0.
59. Li D, Wang D, Liu H *et al.* LEM domain containing 1 (LEMD1) transcriptionally activated by SRY-related high-mobility-group box 4 (SOX4) accelerates the progression of colon cancer by up-regulating phosphatidylinositol 3-kinase (PI3K)/protein kinase B

Downloaded from https://academic.oup.com/pcm/article/7/4/pbae026/7816374 by guest on 04 December 2025

(Akt) signaling pathway. *Bioengineered* 2022;**13**:8087–100. https://doi.org/10.1080/21655979.2022.2047556.
60. Sarrazin S, Adam E, Lyon M *et al.* Endocan or endothelial cell specific molecule-1 (ESM-1): a potential novel endothelial cell marker and a new target for cancer therapy. *Biochim Biophys Acta* 2006;**1765**:25–37. https://doi.org/10.1016/j.bbcan.2005.08.004.
61. Calderaro J, Meunier L, Nguyen CT *et al.* ESM1 as a Marker of Macrotrabecular-Massive Hepatocellular Carcinoma. *Clin Cancer Res* 2019;**25**:5859–65. https://doi.org/10.1158/1078-0432.CCR-19-0859.
62. Liu W, Yang Y, He B *et al.* ESM1 promotes triple-negative breast cancer cell proliferation through activating AKT/NF-κB/Cyclin D1 pathway. *Ann Transl Med* 2021;**9**:533. https://doi.org/10.21037/atm-20-7005.
63. Cui Y, Guo W, Li Y *et al.* Pancancer analysis identifies ESM1 as a novel oncogene for esophageal cancer. *Esophagus* 2021;**18**:326–38. https://doi.org/10.1007/s10388-020-00796-9.
64. Xu H, Chen X, Huang Z. Identification of ESM1 overexpressed in head and neck squamous cell carcinoma. *Cancer Cell Int* 2019;**19**:118. https://doi.org/10.1186/s12935-019-0833-y.
65. Lu J, Liu Q, Zhu L *et al.* Endothelial cell-specific molecule 1 drives cervical cancer progression. *Cell Death Dis* 2022;**13**:1043. https://doi.org/10.1038/s41419-022-05501-5.
66. Yang L, Dong Z, Li S *et al.* ESM1 promotes angiogenesis in colorectal cancer by activating PI3K/Akt/mTOR pathway, thus accelerating tumor progression. *Aging (Albany NY)* 2023;**15**:2920–36. https://doi.org/10.18632/aging.204559.
67. Cai L, Leng ZG, Guo YH *et al.* Dopamine agonist resistance-related endocan promotes angiogenesis and cells viability of prolactinomas. *Endocrine* 2016;**52**:641–51. https://doi.org/10.1007/s12020-015-0824-2.
68. Di Martino JS, Mondal C, Bravo-Cordero JJ. Textures of the tumor microenvironment. *Essays Biochem* 2019,**63**:619–29. https://doi.org/10.1042/EBC20190019.
69. Roudnicky F, Poyet C, Wild P *et al.* Endocan is upregulated on tumor vessels in invasive bladder cancer where it mediates VEGF-A-induced angiogenesis. *Cancer Res* 2013;**73**:1097–106. https://doi.org/10.1158/0008-5472.CAN-12-1855.
70. Rocha SF, Schiller M, Jing D *et al.* Esm1 modulates endothelial tip cell behavior and vascular permeability by enhancing VEGF bioavailability. *Circ Res* 2014;**115**:581–90. https://doi.org/10.1161/CIRCRESAHA.115.304718.
71. Selvam S, Midhun BT, Bhowmick T *et al.* Bioprinting of exosomes: Prospects and challenges for clinical applications. *Int J Bioprint* 2023;**9**:690. https://doi.org/10.18063/ijb.690.

Downloaded from https://academic.oup.com/pcm/article/7/4/pbae026/7816374 by guest on 04 December 2025

Received 2 August 2024; revised 22 September 2024; accepted 7 October 2024. published 9 October 2024
© The Author(s) 2024. Published by Oxford University Press on behalf of the West China School of Medicine & West China Hospital of Sichuan University. This is an Open Access article distributed under the terms of the Creative Commons Attribution-NonCommercial License (https://creativecommons.org/licenses/by-nc/4.0/), which permits non-commercial re-use, distribution, and reproduction in any medium, provided the original work is properly cited. For commercial re-use, please contact journals.permissions@oup.com